

Dataset Paper

Long-Term Aerosol Climate Data Record Derived from Operational AVHRR Satellite Observations

P. K. Chan,¹ X.-P. Zhao,² and A. K. Heidinger³

¹ *Cooperative Institute for Climate and Satellites at North Carolina State University (CICS-NC) and (NCDC), NOAA/NESDIS, 151 Patton Avenue, Asheville, NC 28801, USA*

² *National Climatic Data Center (NCDC), NOAA/NESDIS, 151 Patton Avenue, Asheville, NC 28801, USA*

³ *Center for Satellite Applications and Research (STAR), NOAA/NESDIS, 1225 West Dayton, Madison, WI 53706, USA*

Correspondence should be addressed to X.-P. Zhao; xuepeng.zhao@noaa.gov

Received 13 July 2012; Accepted 23 September 2012

Academic Editors: J. Burkhardt, T. Hussein, A. R. Lupo, and S. Takahama

Copyright © 2013 P. K. Chan et al. This is an open access article distributed under the Creative Commons Attribution License, which permits unrestricted use, distribution, and reproduction in any medium, provided the original work is properly cited.

Aerosol optical thickness (AOT) was retrieved using the Advanced Very High Resolution Radiometer (AVHRR) PATMOS-x Level-2b gridded radiances and the two-channel algorithm of the National Climatic Data Center (NCDC). The primary retrieval product is AOT at 0.63 μm channel. AOT is also retrieved at 0.83 μm or 1.61 μm channel for consistent check. The retrieval was made during day time, under clear sky and snow-free conditions, and over the global oceans. The spatial resolution is 0.1 \times 0.1 degree grid and the temporal resolution is both daily and monthly. The resultant AVHRR AOT climate data record (CDR) spans from August 1981 to December 2009 and provides the longest aerosol CDR currently available from operational satellites. This dataset is useful in studying aerosol climate forcing, monitoring long-term aerosol trends, and evaluating global air pollution and aerosol transport models over the global ocean.

1. Introduction

Aerosols affect the climate through direct and indirect effects. For example, they affect the surface and atmospheric radiation budgets directly through scattering and absorbing shortwave radiation [1, 2]. They also affect climate indirectly through the interaction with clouds and precipitation in a number of intricate ways [3, 4]. Uncertainty in aerosol effects on climate is one of the largest uncertainties in climate forcing [5]. A long-term aerosol dataset with climate quality is essential in reducing the uncertainty of aerosol effect on climate. Satellite remote sensing of aerosols is the only way to provide aerosol data coverage over the globe for multidecadal time periods [6, 7].

Advanced Very High Resolution Radiometer (AVHRR) measurement is the longest operational global satellite observation of the Earth's atmosphere and surface. Observed radiances/reflectances have been widely used to derive long-term products of atmospheric variables, such as cloud and aerosol (see, e.g., [8–12]). AVHRR radiances have been carefully recalibrated recently using more accurate Moderate

Resolution Imaging Spectroradiometer (MODIS) radiances to achieve a better quality [13–15]. The newly calibrated radiances are aggregated into 0.1 \times 0.1 degree orbital grid in the AVHRR Pathfinder Atmospheric Extended (PATMOS-x) Level-2b climate data product [14]. Using the AVHRR PATMOS-x Level-2b top of atmosphere (TOA) radiances and the two-channel aerosol retrieval algorithm [12, 16] of the National Climatic Data Center (NCDC), aerosol optical thickness (AOT) has been retrieved over global oceans from August 1981 to December 2009, which forms the longest aerosol CDR currently available from operational satellites. The product is named NCDC version 2 aerosol CDR product and will be available for public access soon through the official NCDC CDR Web portal (available now through FTP by request from the authors). This paper introduces this version 2 aerosol CDR data product.

2. Methodology

To facilitate the derivation of atmospheric CDRs from AVHRR PATMOS data, more accurate MODIS [17] radiances

have been used to recalibrate the AVHRR radiance retrospectively. NCDC two-channel aerosol retrieval algorithm is used to process PATMOS-x Level-2b TOA clear-sky radiances for global oceanic aerosol retrieval. The algorithm provides estimates of AOT independently in the AVHRR channels at $0.63\ \mu\text{m}$, $0.83\ \mu\text{m}$, or $1.61\ \mu\text{m}$, assuming that the molecular atmosphere, the aerosol microphysics, and surface reflectance are known and invariant. Considering that $1.61\ \mu\text{m}$ channel is only available after 1998 on AVHRR version 3 and the measurement in broad $0.83\ \mu\text{m}$ channel is contaminated by water vapor absorption [16], only AOT retrieved from $0.63\ \mu\text{m}$ channel is served as an AOT long-term CDR.

In operation, the relationship between AOT and dimensionless reflectance (radiance normalized to solar flux) is described by a four-dimensional look-up table (LUT), pre-calculated for different AOTs and view-sun-azimuth angles using 6S radiative transfer code [18, 19], assuming weak absorbing aerosol model and a bimodal log-normal size distribution. Other parameters specified as input to the LUTs are Lambertian oceanic reflectance with diffuse glint correction to the aerosol phase function. The retrieval is performed under several conditions: (1) solar zenith angle $<70^\circ$ and viewing zenith angle $<60^\circ$ to minimize atmospheric curvature effects, (2) glint angle $>40^\circ$ to avoid sun glint contamination, and (3) relative azimuth angle $>90^\circ$ (the antisolar side of satellite orbit) to include only back scattering. The grid box or pixel is regarded as clear when the PATMOS-x cloud probability is less than 1.0%. The PATMOS-x cloud probability is derived from a Naïve Bayesian Technique [20]. The LUTs are searched in the retrieval to find the best match-up of LUT reflectance with the observed reflectance for an observation grid point (or pixel). The AOT value corresponding to the best match-up of reflectance in the LUT is considered as retrieved AOT. The algorithm has gone through both global and regional validations by comparing with ground truth measurement from AERONET (Aerosol Robotic Network [21]) and other satellite aerosol observations (such as MODIS) (see, e.g., [16, 22–24]).

This version 2 AVHRR aerosol product consists of AVHRR AOT at $0.63\ \mu\text{m}$ and $0.83\ \mu\text{m}$ (or $1.61\ \mu\text{m}$) channels. It was derived from PATMOS-x Level-2b TOA reflectances (or radiances) using a two-channel algorithm [12, 16] of NCDC. The differences of this new version 2 product from previous version product [12] include the following: (1) retrieval is performed on the aggregated orbital grid of 0.1×0.1 degree rather than on pixel level as in version 1; (2) different cloud screening criteria have been tested for the entire CDR time period to minimize cloud contamination in the aerosol retrieval while still retaining the strong aerosol signals. Only AOT at $0.63\ \mu\text{m}$ is served as the official version 2 CDR product, and $0.83\ \mu\text{m}$ (or $1.61\ \mu\text{m}$) AOT is a supplementary product used for consistency check.

The enclosed dataset is a long-term averaged monthly mean AOT ($0.63\ \mu\text{m}$) mapped onto 0.1×0.1 equal angle grid over global oceans. It was derived using the following procedures.

- (1) Perform AOT retrieval over global ocean from daily TOA orbital clear-sky reflectances of PATMOS-x

AVHRR Level-2b product. The AOT product produced from this step is named as daily orbital AOT product.

- (2) Generate daily mean AOT by averaging all daily orbital AOT values in a day for every 0.1×0.1 equal angle grid over the global oceans. The resultant product is named as daily mean AOT product.
- (3) Produce the monthly mean AOT by averaging all daily mean AOT in a month for every grid point from August 1981 to December 2009 (total 341 months). The output is named as monthly mean AOT product.
- (4) Long-term monthly averaged mean AOT product for a selected month of 12 months (e.g., January) is obtained by averaging all the monthly mean AOT for this month from 1981 to 2009 (e.g., 28 monthly mean AOT for January) for every grid point. The enclosed data is stored in the binary format. Each month is a data record with a size of 3601×1801 and arranged sequentially from January to December.
- (5) The full AOT ($0.63\ \mu\text{m}$) CDR version 2 product in NetCDF format will be available soon at the official NCDC CDR Web portal (binary version is available now by request from the authors).

Figure 1(a) is an example of this long-term AOT product, which shows the AOT global distribution. The AOT distribution is mainly zonal, with AOT maximum over the equatorial oceans, Arabian Sea, and the South and East Asian coastal waters and near Indonesia. The AOT maxima over the equatorial Atlantic and the Arabian Sea are due to dust emanating from the nearby deserts; the maxima off the west African coast and Indonesia are due to the emissions from biomass burning; the maxima over the South and East Asian coastal waters are due to anthropogenic aerosols from industrial emissions. Figure 1(b) shows that the dataset produced in the aforementioned processing procedures can be used for studying the AOT long-term trend. AOT increases off the West African coast, over the Arabian Sea, over the South and East Asian coastal waters, and around Indonesia. The increase off the South and East Asian coastal waters is consistent with the economic growth and industrial emission enhancement in India and China during the past three decades. The increase near Indonesia and West Africa is due to the increase in biomass burning. The negative trend in the Mediterranean Sea is due to tight emission regulations in the European countries implemented in the past two decades.

A number of natural and anthropogenic events that significantly increase AOT can also be seen clearly in the dataset produced in the previous data-processing procedures. One example is the Pinatubo volcano eruption in the Philippines in June 1991. Figure 2(a) shows that the AOT over the global oceans has increased significantly 3 months after the eruption. Most parts of the equatorial ocean (10°S – 10°N) have AOT exceeding 0.4 (Figure 2(a)), which is more than double of its climatological (or long-term averaging) value (see Figure 2(b)).

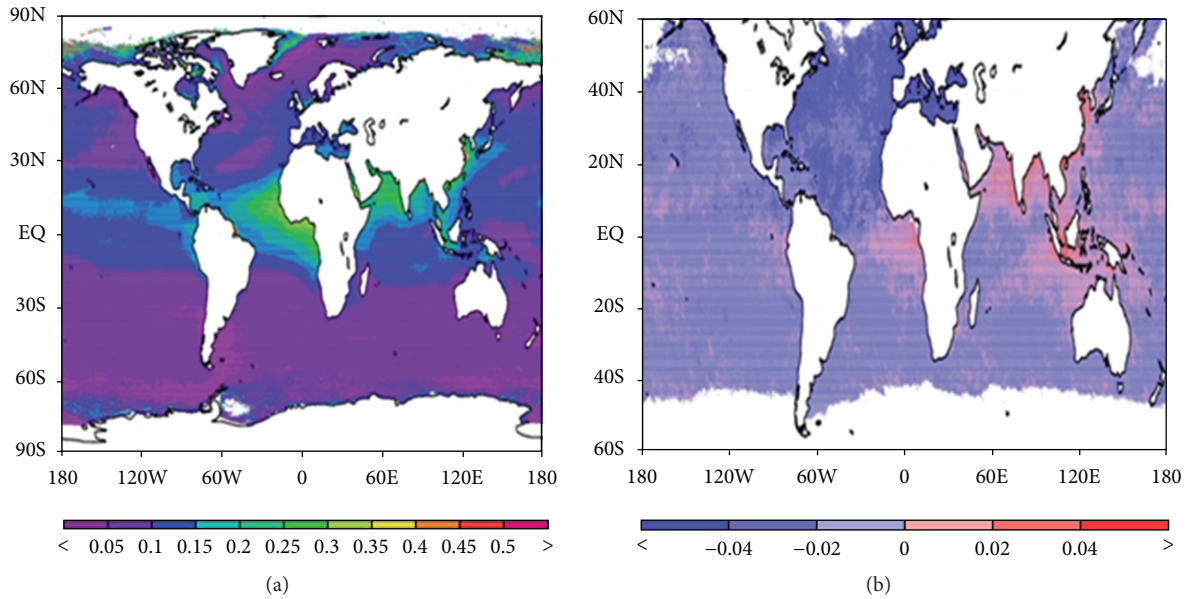


FIGURE 1: (a) Global distribution of long-term averaged AVHRR AOT at $0.63 \mu\text{m}$. (b) Global distribution of AOT trend during 1981–2009 (unit per decade).

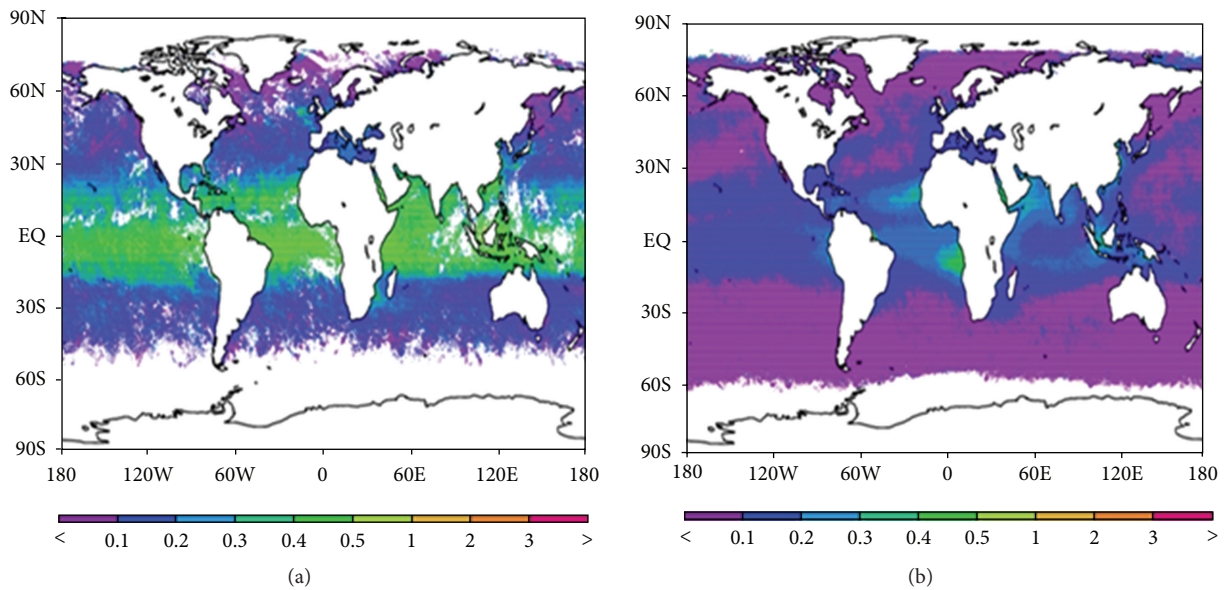


FIGURE 2: (a) Monthly mean AOT ($0.63 \mu\text{m}$) distribution for September 1991 (after the Pinatubo eruption in June 1991). (b) Corresponding distribution for September AOT climatology (August 1981–December 2009).

Figure 3(a) shows the impact of forest fires on the AOT over the oceans surrounding Indonesia in the fall of 1997. The corresponding climatological AOT distribution is given in Figure 3(b) for a comparison. During El-Niño years, the number of forest fires in Indonesia increases significantly. The year 1997 is a strong El-Niño year, and most parts of Indonesia are very dry. In the fall of 1997, the forest fires in Indonesia spread thick clouds of smoke and haze to neighboring countries and the Indian Ocean. In October 1997, a large part of the ocean around Indonesia had AOT exceeding 0.5

(Figure 3(a)) while the corresponding climatological values are generally below 0.4 (Figure 3(b)).

The aerosol CDR dataset produced in the data processing introduced previously has been used to study long-term aerosol trends and climate forcing [12].

3. Dataset Description

The dataset associated with this Dataset Paper consists of 2 items which are described as follows.

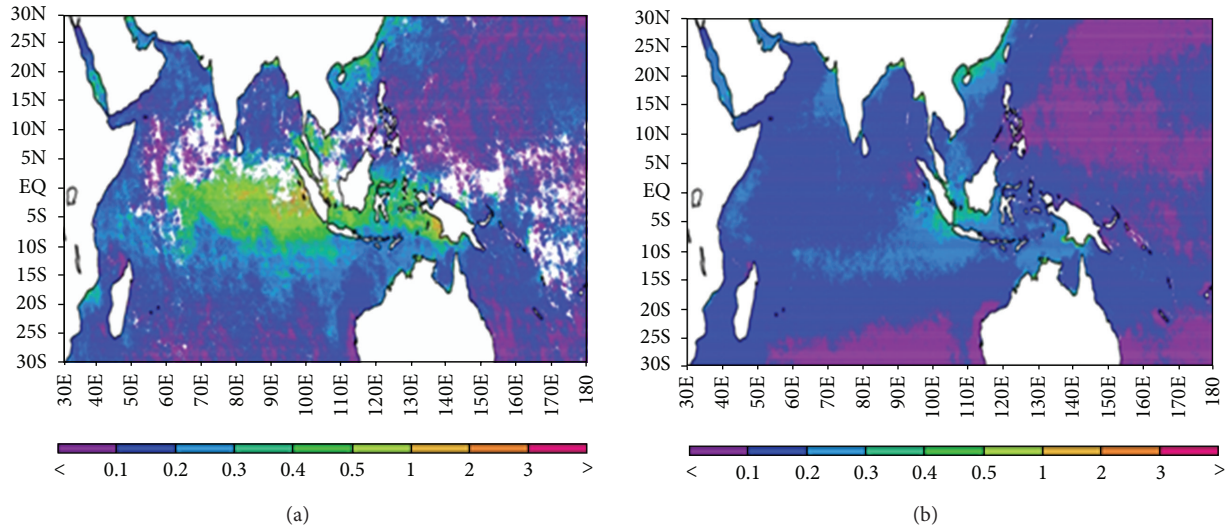


FIGURE 3: (a) October 1997 AVHRR AOT at $0.63 \mu\text{m}$ during the Indonesian forest fire events. (b) Corresponding October AOT climatology (August 1981–December 2009).

Dataset Item 1 (Binary Data). A long-term monthly averaged mean AVHRR aerosol optical thickness ($0.63 \mu\text{m}$) mapped onto 0.1×0.1 equal angle grid over global oceans. The monthly averaged data is averaged for 29 years (1981–2009) for each month. For example, averaged January value is obtained by averaging 29 January values. First data record is January, second is February, and last is December. The center of the first grid box is -180.0E and 90.0S with grid indices increasing eastwards and northwards. Each month is a data record with a size of 3601×1801 and arranged sequentially from January to December. The enclosed data is stored in the binary format and can be plotted by either GRADS or IDL.

Dataset Item 2 (Source Code). IDL code used to read long-term monthly averaged AVHRR aerosol optical thickness data in a binary file (.bin) and output in a spreadsheet file (.dat).

4. Concluding Remarks

There are four major error sources in the AVHRR aerosol retrieval. They are errors in the treatment of surface boundary conditions [16], assumptions about component aerosol microphysical properties [23], inaccurate instrument calibration [12], and incomplete cloud screening [24]. Spurious AOT trends may result from these error sources [25]. In the past decade, significant efforts have been made to minimize these errors (see the previous listed references for more detailed discussions). Optimal cloud-screening criteria have been specifically identified through several sensitivity studies for the whole 29-year AVHRR data record and applied to the production of this version 2 data, which is the major enhancement to this version of the data product compared to the previous versions. A separate paper is being prepared to discuss these sensitivity studies on cloud screening and the improvement in the AOT retrieval. Moreover, vigorous

consistent checks and quality controls have been performed to remove the spurious retrievals and homogenize the AOT product.

The final AOT CDR product is AOT at $0.63 \mu\text{m}$ channel with supplementary AOT at $0.83 \mu\text{m}$ or $1.61 \mu\text{m}$ channel for QC/QA purpose. The spatial resolution of the product is 0.1×0.1 degree grid, and the temporal resolution is both daily and monthly. The data spans from August 1981 to December 2009 and provides the longest aerosol CDR currently available from operational satellites. It can be used for studying aerosol climate forcing, monitoring long-term aerosol trends, and evaluating global air pollution and aerosol transport models over the ocean.

Dataset Availability

The dataset associated with this Dataset Paper is dedicated to the public domain using the CC0 waiver and is available at <http://dx.doi.org/10.7167/2013/140791/dataset>.

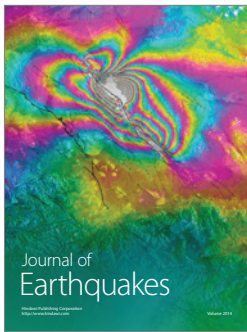
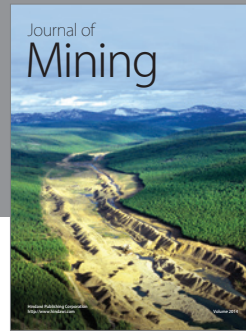
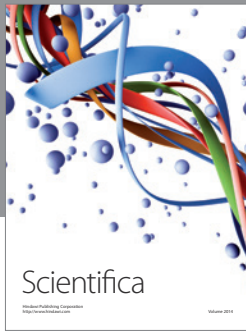
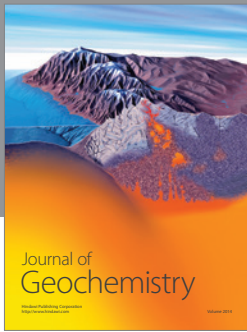
Acknowledgments

The authors would like to acknowledge the NCDC CDR program for providing the funding support to this work. Constructive comments and suggestions from four editors are greatly appreciated. The views, opinions, and findings contained in this report are those of the author(s) and should not be construed as an official National Oceanic and Atmospheric Administration or U.S. Government position, policy, or decision.

References

- [1] A. Ohmura, "Observed decadal variations in surface solar radiation and their causes," *Journal of Geophysical Research*, vol. 114, Article ID D00D5, 9 pages, 2009.

- [2] M. Wild, B. Trüssel, A. Ohmura et al., “Global dimming and brightening: an update beyond 2000,” *Journal of Geophysical Research*, vol. 114, no. 10, Article ID D00D13, 14 pages, 2009.
- [3] P. V. Hobbs, *Aerosol-Cloud-Climate Interactions*, Academic Press, San Diego, Calif, USA, 1993.
- [4] U. Lohmann and J. Feichter, “Global indirect aerosol effects: a review,” *Atmospheric Chemistry and Physics*, vol. 5, no. 3, pp. 715–737, 2005.
- [5] IPCC, *Climate Change 2007: The Physical Science Basis*, New York, NY, USA, 2007.
- [6] M. D. King, Y. J. Kaufman, D. Tanré, and T. Nakajima, “Remote sensing of tropospheric aerosols from space: past, present, and future,” *Bulletin of the American Meteorological Society*, vol. 80, no. 11, pp. 2229–2259, 1999.
- [7] M. I. Mishchenko, I. V. Geogdzhayev, B. Cairns et al., “Past, present, and future of global aerosol climatologies derived from satellite observations: a perspective,” *Journal of Quantitative Spectroscopy and Radiative Transfer*, vol. 106, no. 1–3, pp. 325–347, 2007.
- [8] A. Higurashi and T. Nakajima, “Development of a two-channel aerosol retrieval algorithm on a global scale using NOAA AVHRR,” *Journal of the Atmospheric Sciences*, vol. 56, no. 7, pp. 924–941, 1999.
- [9] M. I. Mishchenko, I. V. Geogdzhayev, B. Cairns, W. B. Rossow, and A. A. Lacis, “Aerosol retrievals over the ocean by use of channels 1 and 2 AVHRR data: sensitivity analysis and preliminary results,” *Applied Optics*, vol. 38, no. 36, pp. 7325–7341, 1999.
- [10] A. K. Heidinger and M. J. Pavolonis, “Global daytime distribution of overlapping cirrus cloud from NOAA’s Advanced Very High Resolution Radiometer,” *Journal of Climate*, vol. 18, no. 22, pp. 4772–4784, 2005.
- [11] M. I. Mishchenko, I. V. Geogdzhayev, W. B. Rossow et al., “Long-term satellite record reveals likely recent aerosol trend,” *Science*, vol. 315, no. 5818, p. 1543, 2007.
- [12] T. X. P. Zhao, I. Laszlo, W. Guo et al., “Study of long-term trend in aerosol optical thickness observed from operational AVHRR satellite instrument,” *Journal of Geophysical Research*, vol. 113, no. 7, Article ID D07201, 14 pages, 2008.
- [13] A. K. Heidinger, C. Cao, and J. T. Sullivan, “Using Moderate Resolution Imaging Spectrometer (MODIS) to calibrate advanced very high resolution radiometer reflectance channels,” *Journal of Geophysical Research*, vol. 107, no. 23, Article ID 4702, 10 pages, 2002.
- [14] A. K. Heidinger, W. C. Straka, C. C. Molling, J. T. Sullivan, and X. Q. Wu, “Deriving an inter-sensor consistent calibration for the AVHRR solar reflectance data record,” *International Journal of Remote Sensing*, vol. 31, no. 24, pp. 6493–6517, 2010.
- [15] C. Cao, M. Weinreb, and H. Xu, “Predicting simultaneous nadir overpasses among polar-orbiting meteorological satellites for the intersatellite calibration of radiometers,” *Journal of Atmospheric and Oceanic Technology*, vol. 21, no. 4, pp. 537–542, 2004.
- [16] T. X. P. Zhao, O. Dubovik, A. Smirnov et al., “Regional evaluation of an advanced very high resolution radiometer (AVHRR) two-channel aerosol retrieval algorithm,” *Journal of Geophysical Research*, vol. 109, no. 2, Article ID D02204, 13 pages, 2004.
- [17] M. D. King, W. P. Menzel, Y. J. Kaufman et al., “Cloud and aerosol properties, precipitable water, and profiles of temperature and water vapor from MODIS,” *IEEE Transactions on Geoscience and Remote Sensing*, vol. 41, no. 2, pp. 442–458, 2003.
- [18] E. F. Vermote, D. Tanré, J. L. Deuzé, M. Herman, and J. J. Morcrette, “Second simulation of the satellite signal in the solar spectrum, 6S: an overview,” *IEEE Transactions on Geoscience and Remote Sensing*, vol. 35, no. 3, pp. 675–686, 1997.
- [19] E. F. Vermote, D. Tanre, J. L. Deuze, M. Herman, and J. J. Morcrette, 6S User Guide Version 2. p. 218, 1997.
- [20] A. K. Heidinger, A. T. Evan, and M. J. Foster, “A naive Bayesian cloud-detection scheme derived from CALIPSO and applied withing PATMOS-x,” *Journal of Applied Meteorology and Climatology*, vol. 51, no. 6, pp. 1129–1144, 2012.
- [21] B. N. Holben, T. F. Eck, I. Slutsker et al., “AERONET—a federated instrument network and data archive for aerosol characterization,” *Remote Sensing of Environment*, vol. 66, no. 1, pp. 1–16, 1998.
- [22] T. X. P. Zhao, L. L. Stowe, A. Smirnov, D. Crosby, J. Sapper, and C. R. McClain, “Development of a global validation package for satellite oceanic aerosol optical thickness retrieval based on AERONET observations and its application to NOAA/NESDIS operational aerosol retrievals,” *Journal of the Atmospheric Sciences*, vol. 59, no. 3, pp. 294–312, 2002.
- [23] T. X. P. Zhao, I. Laszlo, P. Minnis, and L. Remer, “Comparison and analysis of two aerosol retrievals over the ocean in the Terra/Clouds and the Earth’s Radiant Energy System—Moderate Resolution Imaging Spectroradiometer single scanner footprint data: 1. Global evaluation,” *Journal of Geophysical Research*, vol. 110, no. 21, Article ID D21208, 15 pages, 2005.
- [24] T. X. P. Zhao, I. Laszlo, P. Minnis, and L. Remer, “Comparison and analysis of two aerosol retrievals over the ocean in the Terra/Clouds and the Earth’s Radiant Energy System—Moderate Resolution Imaging Spectroradiometer single scanner footprint data: 2. Regional evaluation,” *Journal of Geophysical Research*, vol. 110, no. 21, Article ID D21209, 18 pages, 2005.
- [25] Z. Li, X. Zhao, R. Kahn et al., “Uncertainties in satellite remote sensing of aerosols and impact on monitoring its long-term trend: a review and perspective,” *Annales Geophysicae*, vol. 27, no. 7, pp. 2755–2770, 2009.



Hindawi

Submit your manuscripts at
<http://www.hindawi.com>

